Rational Billiards

How to Win Every Pentagonal Pool Game

Caden Ruan

July 2025

1 Introduction

In the 1400s, King Louis XI of France was recorded to possess the first indoor billiard table, transforming the game of pool into an indoor sport. Around 600 years later, Alexander Zelyakov and Anatole Katok published their paper "Topological transitivity of billiards in polygons", widely considered to be the first mathematical paper which formalized rational billiards as a topic.

Now, how does the recreational game of pool relate to this topic of rational billiards? Many readers are already familiar with 8-ball pool before, whether on a real table or on a phone. One of the most satisfying aspects of pool is the ability to perfectly control the trajectory of the cue ball. The cue ball will roll in a straight line until it hits a pool table wall, where it'll bounce off at the same angle which it hit it with. On a phone screen, one could even imagine pulling out a ruler to carefully measure each angle and trajectory, calculating the perfect shot in every round of 8-ball pool.

Mathematically, these rules and ideas lead to the study of billiard dynamics, which analyzes how a frictionless ball moves forever in a closed polygon, bouncing perfectly off the sides each time. One main question posed in billiard dynamics is the concept of periodic billiard paths; Will the ball you launch ever return to exactly where it started, moving in the same direction?

For common shapes like squares or rectangles, billiard trajectories insides these polygons are well understood. It's known that if a ball's direction has a rational slope, its path will always repeat after a certain amount of bounces. Billiard trajectories in shapes like triangles have been well-explored similarly. In 2009, Richard Evan Schwartz proved that all triangles with angles at most 100 degrees contain a periodic billiard path, and this number has since been improved to 112.2 degrees. Billiard trajectories like these can be classified as rational billiards; a special case of billiard systems where all interior angles of the polygon are rational multiples of π.

However, not all rational billiards have solutions like the square or equilateral triangle. The regular pentagon poses a challenge to find periodic paths on. Unlike squares or equilateral triangles, the regular pentagon cannot tile a plane completely, meaning the usual trick of unfolding does not produce a simple pattern.

Finally, in 2018, Diana Davis and Samuel Lelièvre made a breakthrough on this problem. They found a way to transform the double pentagon, which is two pentagons stuck together, into a new shape called the golden L, which is a shape constructed using rectangles and the golden ratio, making billiard trajectories easier to calculate. Using this shape, they managed to give a step-by-step method to find every possible periodic billiard path inside the pentagon. They also managed to determine how many times it bounces (the combinatorial period) and how far the ball travels (the Euclidean length) before returning to its original position.

2 Billiards

2.1 Definitions

Definition 2.1. *A **billiard system** is defined as the motion of a point mass inside a closed polygonal region, where the particle moves in straight lines within the interior and reflects elastically off the boundary. The motion is governed by the law of reflection: the angle of incidence equals the angle of reflection.*

Lemma 2.2. *Let a billiard trajectory strike the boundary of a polygonal table at a point where the boundary is smooth. Then the angle of incidence is equal to the angle of reflection; that is, the trajectory satisfies the law*

$$\theta_{in} = \theta_{out},$$

where θ_{in} is the angle between the incoming trajectory and the normal of the boundary, and θ_{out} is the angle between the outgoing trajectory and the same normal.

Proof. Let the billiard ball travel along a straight line segment until it strikes the boundary at a point P. Let the incoming vector $\vec{v}_{\text{in}}$ make an angle θ_{in} with the boundary at P.

According to the geometric law of reflection, the reflected vector $\vec{v}_{\text{out}}$ lies in the same plane as $\vec{v}_{\text{in}}$ and $\vec{n}$, and satisfies

$$\vec{v}_{\text{out}} = \vec{v}_{\text{in}} - 2(\vec{v}_{\text{in}} \cdot \vec{n})\vec{n},$$

which is the reflection formula across a plane normal to $\vec{n}$.

This transformation preserves the angle between the trajectory and the boundary, meaning that the angle the outgoing trajectory makes with $\vec{n}$ is equal to that of the incoming trajectory.

$$\text{Therefore, } \theta_{\text{in}} = \theta_{\text{out}}.$$

Hence, the law of reflection holds at every collision with the boundary. □

2.2 Examples of Billiard Systems

2.2.1 Rectangular Billiard (Pool Table)

While playing pool, have you ever felt like Donald Duck?

In Donald in Mathmagic Land (1959), there's a moment where Donald frantically hits the cue ball in every direction, hoping one shot might magically work.

But then, he's introduced to the diamond system, a method for predicting bank shots in pool. Suddenly, the pool table transforms into a game of math, where each shot follows a predictable pattern based on angles and reflections.

This moment perfectly captures rectangular billiards. In mathematics, a standard pool table is modeled as a rectangle where the ball reflects off the sides according to the law of reflection. If the direction of the ball has a rational slope, the path will always repeat itself at one point.

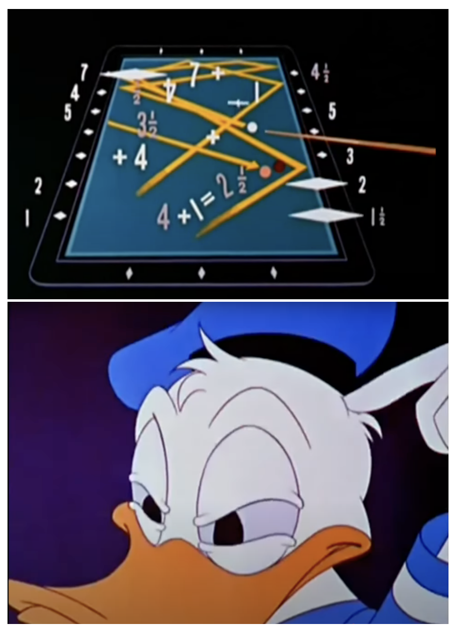

Donald hits the ball at random.

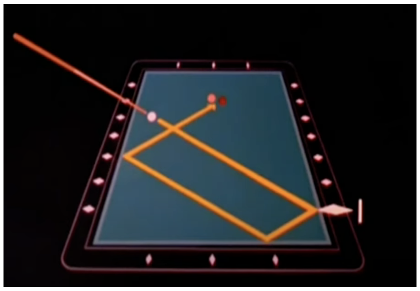

Figure 1: The diamond system saves the day!

Figure 2: Now Donald is happy!

2.2.2 Elliptic Billiard

An elliptic billiard takes place inside an elliptical boundary. A unique feature of this system is that any trajectory starting at one focus will always reflect through the other focus. Elliptic billiards typically exhibit three distinct types of behavior, focal, hyperbolic, and parabolic. In focal trajectories, the trajectories pass through both foci and reflect back and forth and this motion will converge to the major axis. In hyperbolic trajectories, the trajectories bounce around creating a dense hyperbolic-shaped region in between the foci. In elliptic trajectories, the trajectories bounce around creating a dense elliptic-shaped region outside the foci.

Will insert image of the three kinds of billiards

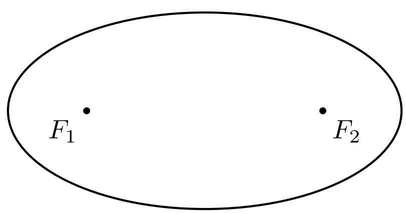

Figure 3: Three types of trajectories in an elliptic billiard: focal (blue), hyperbolic (red), and parabolic (green).

2.2.3 Sinai Billiard

The Sinai billiard, also known as the Lorentz gas, involves a square domain with a circular obstacle removed from the center. This system is one of the earliest known models of deterministic chaos. Despite the simple geometry, slight changes in initial conditions of the particle trajectory lead to significant changes in behavior.

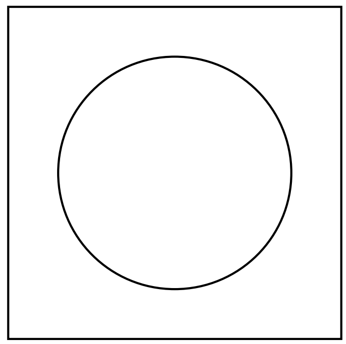

Figure 4: Sinai billiard system: square boundary with a central circular obstacle

3 Rational Billiards

3.1 Definitions

Definition 3.1. *A* rational polygon *is a polygon where each of its interior angles is a rational multiple of π. That is, for each interior angle θ_i, there exist integers m_i, n_i such that $\theta_i = \frac{m_i \pi}{n_i}$.*

Definition 3.2. *A* rational billiard *is a billiard system in which the polygonal domain is a rational polygon.*

3.2 Examples

The class of rational billiards is particularly important due to the structure it imposes on the billiard system. When the underlying polygon is rational, the dynamics of the billiard flow become far more easy to calculate as the possible directions of motion are limited and we are able to use techniques such as unfolding.

Several classic shapes qualify as rational polygons and serve as foundational examples.

- In a **square** table, all angles are $\pi/2$
- In an **equilateral triangle**, all angles are $\pi/3$

- In a **regular hexagon**, all angles are $2\pi/3$

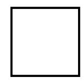

(a) Square

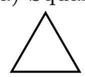

(b) Equilateral Triangle

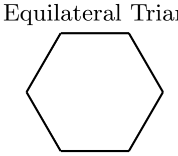

(c) Regular Hexagon

Figure 5: Trajectories in three basic rational billiard tables. (Will add trajectories later when I figure it out and its vertical for some reason fix this using a table and alignment)

These cases contrast sharply with irrational polygons, where the internal angles are not rational multiples of π. In such settings, trajectories often behave erratically, and no unfolding procedure exists, leading to unpredictable billiard trajectories.

4 Periodic Trajectories in Billiards

4.1 Definitions and Properties

In the study of billiards, one central object of interest is the periodic trajectory.

Definition 4.1. *A billiard trajectory is said to be* periodic *if the particle returns to its initial position and direction after a finite number of reflections off the boundary. That is, a trajectory starting at a point x_0 with initial direction θ is periodic if there exists a minimal integer n such that the path after n reflections returns to x_0 with the same incoming direction θ.*

One example of a periodic trajectory lies in a square billiard table. In a square billiard table, if the slope of the trajectory is rational, say $m = p/q$, then the trajectory is periodic, and the particle will return to its initial position in $2(p+q)$ reflections off the boundary. In the following section, we will prove this claim.

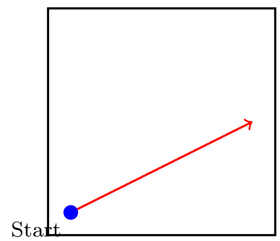

Figure 6: A periodic trajectory in a square billiard with rational slope $\frac{1}{2}$. (Not complete yet)

Not all trajectories in a billiard table are periodic; some fill regions densely, never returning exactly to their starting point.

4.2 Periodic Paths in Classical Shapes

Acute Triangle: The Fagnano Orbit

One classical polygon which exhibit periodic orbits is the *Fagnano orbit* in acute triangles, which exists in any acute triangle and is the shortest periodic billiard path in all acute triangles.

Proof. Let $\triangle ABC$ be an acute triangle. Let D, E, F be the feet of the perpendiculars from vertices A, B, C to the opposite sides BC, AC, AB, respectively. Consider the path $D \to E \to F \to D$.

To prove that this forms a valid billiard trajectory, we must show that the path reflects off the sides of the triangle according to the law of reflection: the angle of incidence equals the angle of reflection.

We use a geometric argument based on reflection and similar triangles. Consider the segment $\overrightarrow{DE}$, which reflects off side AC at point E. Reflect the triangle $\triangle ABC$ across the line AC, and let D' be the reflection of point D. Since E lies on the mirror line AC, the path $D \to E \to F$ becomes a straight-line path $D' \to E \to F$ in the reflected triangle.

The triangle $\triangle D'EF$ is thus a straight-line path, and the point E lies on the reflection line. By construction, the triangles $\triangle D'EA$ and $\triangle DEA$ are congruent by the Hypotenuse-Leg (HL) criterion, since both share the segment AE and include right angles at E. It follows that the angle between $\overrightarrow{DE}$ and side AC is equal to the angle between $\overrightarrow{EF}$ and side AC, confirming that the angle of incidence equals the angle of reflection at point E.

An identical argument applies at points F and D, demonstrating that each leg of the path reflects off its respective side in accordance with the law of reflection. Since the triangle is acute, all three altitudes fall within the triangle, ensuring that the path lies entirely within the interior.

After three such reflections, the trajectory returns to its starting point D with the same direction, forming a closed periodic billiard orbit of period 3. This trajectory is known as the *Fagnano orbit*, and it is also the shortest periodic path that can be inscribed within the triangle. □

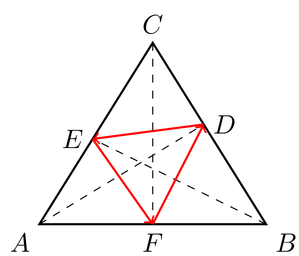

Figure 7: Fagnano periodic orbit inside an acute triangle.

4.3 Research into Non-classical Shapes and Difficulties

While classical billiard theory largely concerns rational polygons, recent efforts have explored more general domains, such as those with curved boundaries or irrational angles. These non-classical shapes present major theoretical and computational challenges, especially regarding the existence and classification of periodic orbits.

A central example is the Sinai billiard, which consists of a square with a circular obstacle removed from its center. First studied by Yakov Sinai in the 1960s, this model exhibits chaotic and ergodic behavior, in stark contrast to the structured dynamics seen in rational polygons. The presence of a convex obstacle introduces dispersing reflections, preventing the trajectory from settling into periodic patterns or invariant cylinders. As a result, tools like unfolding and translation surfaces—essential in rational polygonal billiards—do not apply in this setting.

Even in purely polygonal domains, challenges persist. One long-standing open question is whether every triangle admits a periodic billiard trajectory. While rational triangles (those with all angles rational multiples of π) are known to admit periodic orbits due to unfolding methods, the general case remains elusive. The most notable progress has come from computer-assisted proofs by Richard Schwartz and collaborators, who have confirmed that all triangles with largest angle less than 112.3° possess at least one periodic trajectory. Beyond this angle, the question is unresolved.

These limitations underscore the fragility of periodicity under geometric perturbation. Small deviations from rationality or the introduction of curvature can destroy the combinatorial structures (e.g., cutting sequences, saddle connection trees) that organize periodic directions in rational billiards. Consequently, research into non-classical shapes often relies on numerical experiments, heuristics, and partial results, highlighting a rich area where dynamical systems theory, geometry, and computation intersect.

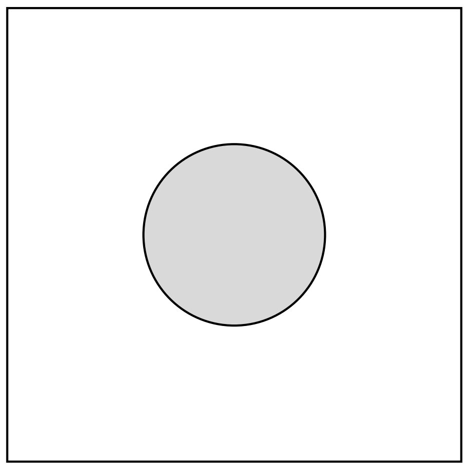

Figure 8: The Sinai Billiard

5 Unfolding Method and Translation Surfaces

5.1 Unfolding

Zemlyakov and Katok established that rational billiards can be studied through the symmetries generated by reflecting the polygon across its sides, a process known as unfolding. This symmetry gives rise to a reflection group and allows one to construct covering surfaces that simplify the analysis of billiard trajectories.

The sequence of reflections forms a finite group, known as the *reflection group*, which governs the structure of the unfolding. When the group is finite, one can construct a compact translation surface by appropriately gluing together a finite number of polygonal copies. On this surface, the billiard flow corresponds to straight-line motion—thus transforming a piecewise-dynamical system with reflections into a flow on a flat Riemann surface with conical singularities.

This technique not only simplifies the analysis of trajectories but also allows the application of tools from geometry and topology. For example, on the unfolded surface, trajectories can be studied using holonomy vectors, saddle connections, and affine automorphisms. The genus of the resulting surface depends on the angles of the original polygon and increases with the complexity of the reflection group. A classical example is the square billiard, which unfolds into a torus tiled by four copies of the square. In contrast, the regular pentagon unfolds into a higher-genus surface composed of ten pentagons arranged in a necklace pattern.

Unfolding also plays a central role in defining and analyzing cutting sequences, periodic directions, and Veech groups. For rational polygons, this connection enables the enumeration of periodic trajectories and the classification of directions into minimal, uniquely ergodic, or periodic types. However, this approach critically depends on the rationality of the angles; for irrational polygons, the unfolding generally fails to produce a translation surface, making the dynamics much harder to understand.

Thus, unfolding serves as a bridge between polygonal billiards and the rich world of flat surfaces and Teichmüller dynamics, enabling deep structural insights that would be inaccessible through direct analysis of the original billiard system.

5.2 Translation Surfaces

6 The Pentagon Problem

6.1 Introduction to the Pentagon

The regular pentagon presents a challenging yet compelling case in the study of polygonal billiards. Unlike polygons that tile the plane by reflections (e.g., squares, equilateral triangles), the pentagon lacks many symmetries which lie in these polygons despite it being a rational billiard. As a result, regular pentagons do not tile the plane evenly. Remarkably, periodic trajectories do exist in the pentagon, but their structure is far more subtle and beautiful than in simpler shapes.

6.2 Results of Davis and Lelièvre Breakthrough

Davis and Lelièvre developed a powerful framework to understand periodic trajectories in the regular pentagon using translation surfaces. By unfolding the

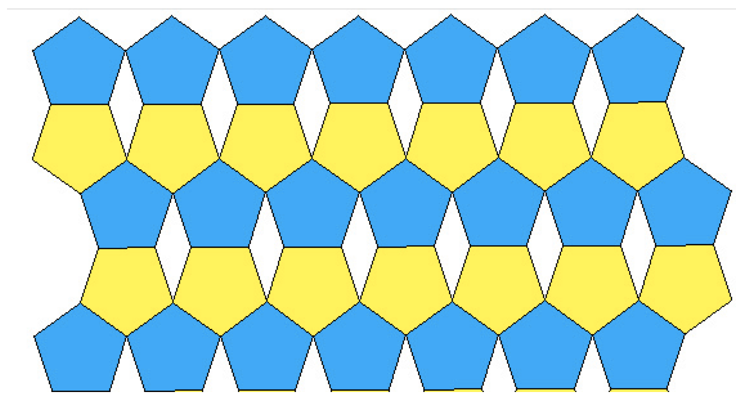

Figure 9: Incomplete tiling of the plane using regular pentagons

pentagon through reflections, they constructed the *necklace* surface consisting of ten pentagons. This necklace surface covers the *double pentagon* surface (built from two oppositely-oriented pentagons), which in turn is affinely equivalent to a much simpler surface: the *golden L*. Working on the golden L, a right-angled surface with affine symmetries, allows for exact enumeration of periodic directions via a tree structure. Each periodic trajectory in the pentagon corresponds to a saddle connection vector on the golden L, and the dynamics can be fully translated between these surfaces.

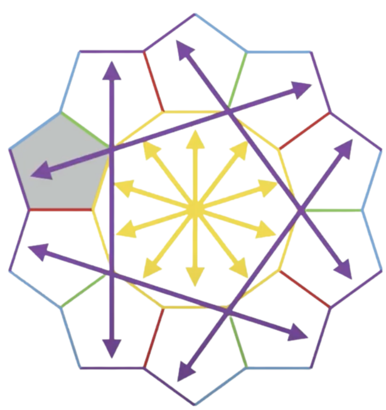

Figure 10: Pentagon Ring

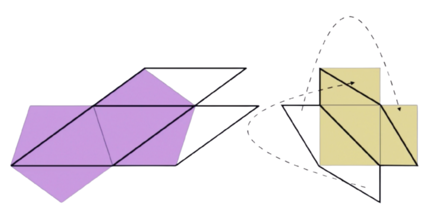

Figure 11: Pentagon to Golden L

7 The Golden L and the Double Pentagon

7.1 Construction of the Golden L

The golden L is constructed from three rectangles: a unit square, a rectangle of size $1 \times \frac{1}{\phi}$, and another of size $\frac{1}{\phi} \times 1$, where $\phi = \frac{1+\sqrt{5}}{2}$ is the golden ratio. These are glued to form an L-shaped translation surface. Through a series of shears and cuts, the golden L can be mapped to the double pentagon surface, which then folds into the necklace and ultimately into the original pentagon billiard table.

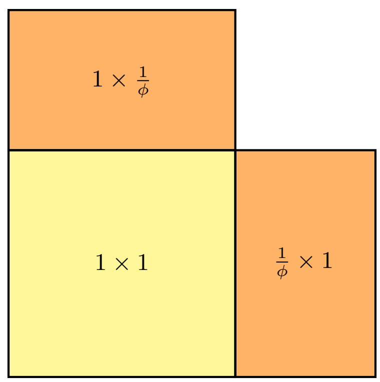

Figure 12: The Golden L

7.2 Geometry of the Golden L

The golden L surface supports two cylinders of periodic trajectories in every periodic direction: a short and a long cylinder, whose length ratio is ϕ. Each cylinder corresponds to a collection of parallel trajectories, and the cylinder decomposition reveals the modular structure of the surface.

To study trajectories in the regular pentagon, we take advantage of the fact that the golden L surface is affinely equivalent to the double pentagon surface. The key transformation is a shear matrix that maps vectors in the golden L to their corresponding directions in the double pentagon. Specifically, this shear is given by:

$$P = \begin{bmatrix} 1 & \cos\left(\frac{\pi}{5}\right) \\ 0 & \sin\left(\frac{\pi}{5}\right) \end{bmatrix}, \quad P^{-1} = \begin{bmatrix} 1 & \cos\left(\frac{\pi}{5}\right) \\ 0 & \sin\left(\frac{\pi}{5}\right) \end{bmatrix}^{-1}$$

As an example, if $\vec{v} = \begin{bmatrix} 1 \\ 1 \end{bmatrix}$ is a vector on the golden L, then its image under the shear is:

$$P \cdot \vec{v} = \begin{bmatrix} 1 & \cos\left(\frac{\pi}{5}\right) \\ 0 & \sin\left(\frac{\pi}{5}\right) \end{bmatrix} \begin{bmatrix} 1 \\ 1 \end{bmatrix} = \begin{bmatrix} 1 + \cos\left(\frac{\pi}{5}\right) \\ \sin\left(\frac{\pi}{5}\right) \end{bmatrix}$$

This affine transformation allows us to transfer geometric and combinatorial information about periodic trajectories from the golden L, where they are easier to describe algebraically, onto the more complex geometry of the double pentagon, and ultimately to the regular pentagon.

8 Tree Structure of Periodic Directions in the Pentagon

8.1 Shears

The golden L admits a decomposition of the first quadrant into four distinct sectors, each of which corresponds to a shear transformation σ_i. These shears act on vectors in the positive cone and generate the Veech group of the surface. The purpose of each σ_i is to map the full first quadrant into one of the four sectors W_1, W_2, W_3, W_4, which tile the quadrant non-overlappingly (as shown in Figure 13).

The matrices are defined as:

$$\sigma_0 = \begin{bmatrix} 1 & \phi \\ 0 & 1 \end{bmatrix}, \quad \sigma_1 = \begin{bmatrix} \phi & \phi \\ 1 & \phi \end{bmatrix}, \quad \sigma_2 = \begin{bmatrix} \phi & 1 \\ \phi & \phi \end{bmatrix}, \quad \sigma_3 = \begin{bmatrix} 1 & 0 \\ \phi & 1 \end{bmatrix}$$

Each matrix is responsible for compressing and redirecting directions into its associated sector. These shears provide a recursive mechanism for constructing periodic directions and serve as the foundation for the tree of saddle connections.

8.2 Tree of Words

Every periodic direction on the golden L surface can be obtained by starting with a known direction—typically the base vector $[1, 0]$—and applying a finite sequence of the shear matrices $\sigma_0, \sigma_1, \sigma_2, \sigma_3$. This recursive process defines a 4-ary tree where each node corresponds to a direction vector, and the path to reach it is recorded as a *tree word*—a sequence of digits encoding the shears applied.

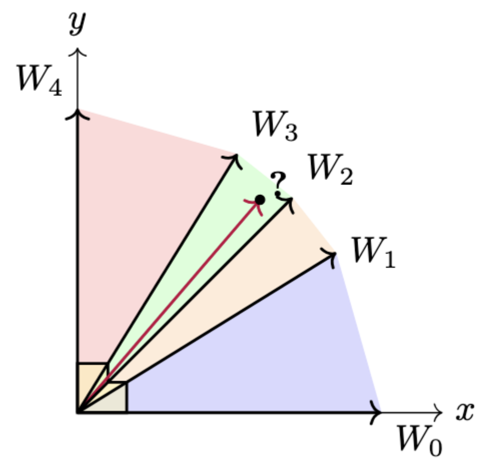

Figure 13: Color coded sectors of the Golden L. Each shear σ_0 to σ_3 maps the positive quadrant into a colored wedge.

For instance, the word 0213 represents the composition $\sigma_0\sigma_2\sigma_1\sigma_3$, applied to the initial vector $[1, 0]$. The resulting vector lies in a specific direction corresponding to a periodic trajectory in the golden L and, via shear conjugation, in the double pentagon.

The tree structure is symmetric about the line $y = x$, and its depth determines the geometric complexity and combinatorial period of the corresponding trajectories.

9 Period of Periodic Trajectories

9.1 Combinatorial Period

One of the key insights of Davis and Lelièvre's work is the ability to compute the combinatorial period of a periodic trajectory directly from the coordinates of its associated saddle connection vector on the golden L surface. These vectors arise from applying sequences of shear matrices to the initial direction $[1, 0]$, forming a tree structure where each path (or "tree word") uniquely determines a direction and its corresponding dynamics.

Theorem 9.1 (Form of Periodic Directions)**.** *Each tree word corresponds to a vector of the form*

$$[a + b\phi,\ c + d\phi],$$

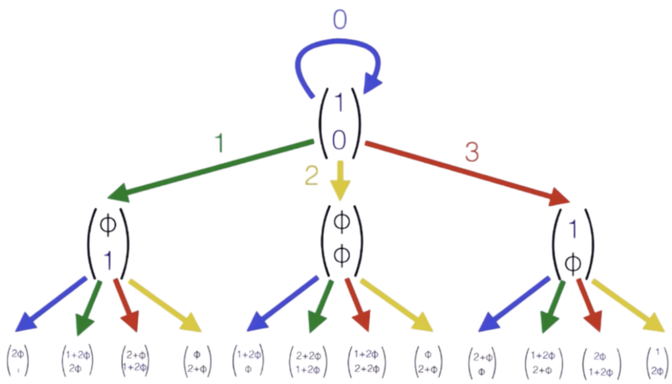

Figure 14: Construction of the tree of directions from the base vector. Arrows represent shear applications.

where $a, b, c, d \in \mathbb{Z}_{\geq 0}$ and $\phi = \frac{1+\sqrt{5}}{2}$ is the golden ratio. This vector encodes the direction of a periodic trajectory on the golden L.

Theorem 9.2 (Combinatorial Period on the Double Pentagon)**.** *Given a tree word that leads to the vector $[a + b\phi, c + d\phi]$, the associated periodic trajectory on the double pentagon has a combinatorial period*

$$P_{double} = 2(a + b + c + d).$$

Theorem 9.3 (Adjustment for Regular Pentagon)**.** *To compute the period on the original regular pentagon, one must determine the symmetry of the trajectory on the double pentagon:*

- *If the trajectory is* ***asymmetric****, then $P_{pentagon} = P_{double}$.*
- *If the trajectory is* ***symmetric****, then $P_{pentagon} = 5 \cdot P_{double}$.*

10 Conclusion and Generalizations

The study of periodic trajectories in the regular pentagon reveals a rich connection between the studies geometry, algebra, and dynamics. Through the lens of translation surfaces and affine shears, Davis and Lelièvre's framework allows one to classify and count periodic directions using tree structures and saddle connection vectors defined in terms of the golden ratio. The golden L surface, serving as a combinatorially and geometrically tractable model, translates the complexities of the regular pentagon into an explicitly computable setting.